LUND UNIVERSITY

Application of fracture mechanics to concrete : summary of a series of lectures 1988

Hillerborg, Arne

1988

Link to publication

Citation for published version (APA):
Hillerborg, A. (1988). *Application of fracture mechanics to concrete : summary of a series of lectures 1988*. (Report TVBM; Vol. 3030). Division of Building Materials, LTH, Lund University.

Total number of authors:
1

General rights
Unless other specific re-use rights are stated the following general rights apply:
Copyright and moral rights for the publications made accessible in the public portal are retained by the authors and/or other copyright owners and it is a condition of accessing publications that users recognise and abide by the legal requirements associated with these rights.
• Users may download and print one copy of any publication from the public portal for the purpose of private study or research.
• You may not further distribute the material or use it for any profit-making activity or commercial gain
• You may freely distribute the URL identifying the publication in the public portal

Read more about Creative commons licenses: https://creativecommons.org/licenses/

Take down policy
If you believe that this document breaches copyright please contact us providing details, and we will remove access to the work immediately and investigate your claim.

LUND UNIVERSITY

PO Box 117
221 00 Lund
+46 46-222 00 00

Download date: 12. Oct. 2024

DIVISION OF BUILDING MATERIALS
LUND INSTITUTE OF TECHNOLOGY

APPLICATION OF FRACTURE MECHANICS TO CONCRETE

Summary of a series of lectures 1988

Arne Hillerborg

REPORT TVBM-3030
LUND SWEDEN 1988

CODEN: LUTVDG/(TVBM-3030)/1-28/(1988)

APPLICATION OF FRACTURE MECHANICS TO CONCRETE

Summary of a series of lectures 1988

Arne Hillerborg

ISSN 0348-7911

REPORT TVBM-3030
LUND SWEDEN 1988

APPLICATION OF FRACTURE MECHANICS TO CONCRETE

with emphasis on the work performed at Lund Inst. of Tech.

Arne Hillerborg, Div. of Building Materials, Lund Inst. of Tech., Lund, Sweden.

Abstract

Different approaches to the application of fracture mechanics to concrete are discussed, with an emphasis on the models based on strain softening and strain localization, particularly the fictitious crack model. Examples of results of the theoretical analyses are demonstrated, and some practical conclusions are drawn. Future research is also commented.

Introduction

Conventional fracture mechanics is mainly based on the theory of elasticity and it is used for studying the stability and propagation of existing cracks. The modern form of application of fracture mechanics to concrete, which was first developed in Lund, differs from the conventional fracture mechanics in both these respects.

In the basic form of conventional fracture mechanics it is assumed that the stresses and strains tend towards infinity at a crack tip, Fig. 1. This is of course not realistic. In spite of this the theoretical results based on this assumption in many cases lead to realistic conclusions. In other cases this is not the case. This has since long been recognized, and in conventional fracture mechanics many methods have been advised to overcome this problem. Some of these methods are similar to the methods now applied to concrete, even though there are fundamental differences.

The most important practical difference between conventional fracture mechanics and the modern application to concrete is that conventional fracture mechanics has never been applied to structures

without any initial crack, whereas the modern model can also be applied to this case. It is now possible not only to study the stability and propagation of a crack, but also its formation. Thus the complete development of fracture can be analysed by means of one model as a continuous process. This is an expansion of fracture mechanics, which opens quite new possibilities to analyse fracture of real structures, as will be demonstrated by means of examples.

This circumstance has been emphasized here, because it has not always been fully appreciated. Thus for example the new approach is sometimes described as a variant of the so called Dugdale-Barenblatt model. Dugdale and Barenblatt never realised the possibility to use this type of model for the analyses of uncracked structures. They only intended their models as explanations of the stress situation in the vicinity of the tip of an existing crack.

Conventional fracture mechanics

As a background for the understanding of the new model a short description will be given of conventional fracture mechanics, particularly linear elatic fracture mechanics, often written LEFM for short.

If a stress is applied perpendicular to a crack with a sharp tip, the linear elastic solution shows that a stress concentration will appear at the tip, such that the stress approaches infinity, Fig. 1. Close to the crack tip the stress distribution is approximately described by the equation

$$\sigma_y = \frac{K}{\sqrt{2\pi x}}$$

In this equation x is the distance from the crack tip and K is called the **stress intensity factor.** This factor can be calculated from the equation

$$K = Y\sigma\sqrt{a}$$

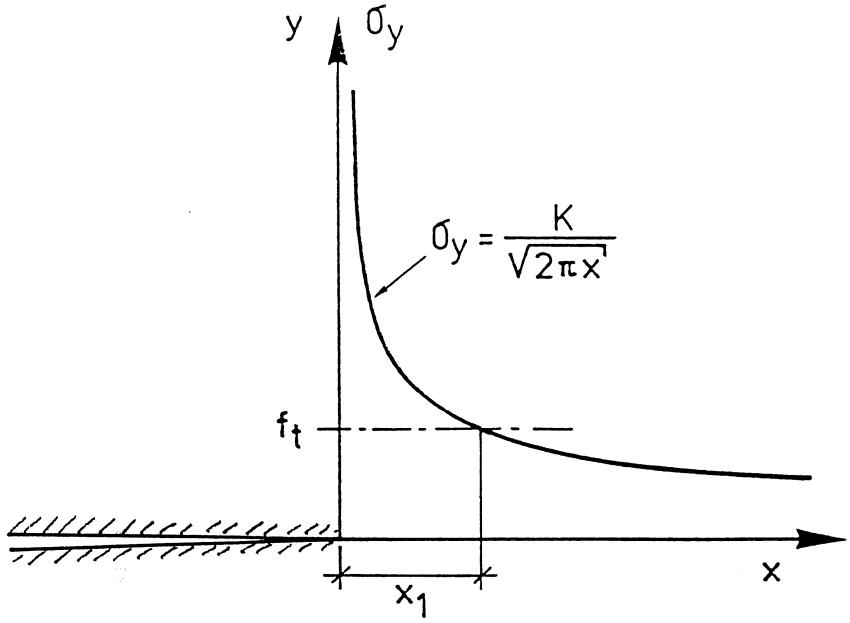

Fig. 1 Stress distribution according to the theory of elasticity.

where a is the crack length (for a crack at an edge, or half the crack length for an interior crack), σ is the stress which would have acted if there had been no crack, and Y is a dimensionless factor, which depends on the type of structure, the loading conditions, and to some extent to the crack length. The value of Y is often approximately 2.

According to this formal stress distribution the stress within a distance x_1 exceeds the tensile strength f_t. The stress distribution cannot be valid within this part. The larger the value is of x_1, the less accurate are the conclusions drawn by means of LEFM.

As the stress approaches infinity, the analysis of crack stability and crack propagation cannot be based on a comparison with the strength of the material. Instead it is necessary to introduce a new criterion, which says that the crack will start propagating when the stress intensity factor K reaches a critical value, **the critical stress intensity K_c**, which is assumed to be a material property.

It can be noticed that conventional fracture mechanics can only treat problems concerned with an existing crack, as K becomes zero when the crack length a is zero. For uncracked material the ordinary theory of strength of materials has to be used, with a comparison

between a stress and a strength as fracture criterion. This means that different models have to be used for cracked and uncracked material, with different fracture criteria and two different material properties, K_c and strength. This lack of continuity is a drawback, at least for materials like concrete.

An alternative treatment according to LEFM is based on the stress release rate when a crack propagates, i e the amount of energy which is released in the structure per unit crack area when the crack propagates. An **energy release rate G** is theoretically calculated. The crack i assumed to propagate if G reaches a critical value, **the critical energy release rate G_c**, which is equal to the amount of energy that is absorbed in the fracture zone per unit area when the crack grows. It can be demonstrated that the approaches by means of stress intensity factors and energy release rates are equivalent, and that they are coupled by means of the following relation for the case of plane stress conditions.

$$K^2 = EG$$

It has long been recognised that the unrealistic assumption that the stress and strain approaches infinity can lead to erroneous results. Many methods are used to make corrections in order to take into account the limited strength of the material. These methods will not be discussed here, as they as a rule give results, which are not accurate enough for concrete structures of normal sizes.

The basis of the new approach.

The basic idea of the new approach is best demonstrated by means of a discussion of the stress-deformation behaviour of a specimen in a tension test, Fig. 2. It is assumed that complete stress-deformation curves are recorded simultaneously by means of four gauges. Gauges B, C, and D are of the same length and situated immediately after each other, whereas gauge A has a length which is equal to the sum of gauges B, C, and D.

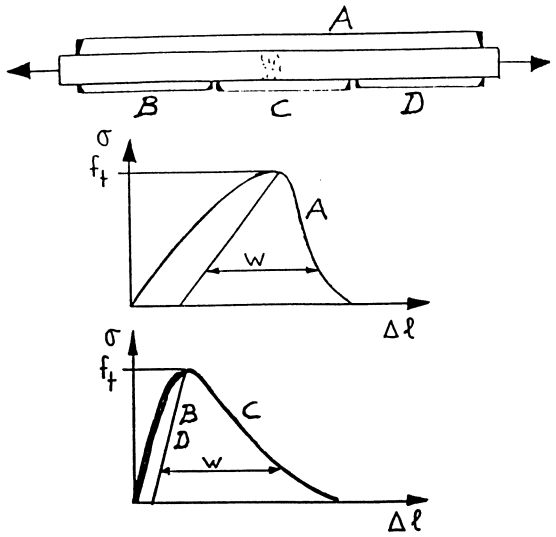

Fig. 2. Deformations along different gauge lengths in a tensile test.

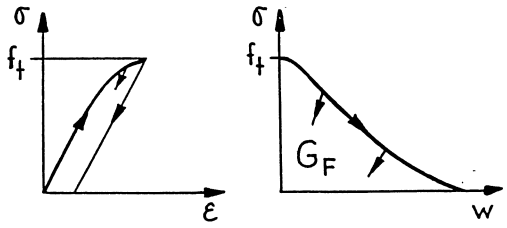

Fig. 3. General deformation properties.

The test is assumed to be performed in deformation control, which means that the deformation is slowly increased. During the first phase of the test, the stress increases as the deformation increases. This is said to be the ascending branch in the stress-deformation diagram. If the specimen is assumed to be homogenuous, the relative elongation during this phase is the same along the whole specimen. This means that the deformation can be described by means of a strain ε, defined as the deformation divided by the gauge length. The same stress-strain diagram is valid for the whole specimen at this stage.

After the peak stress has been reached, the **post-peak** stage, a further increase in deformation means that the stress decreases. We are now on the **descending branch** in the diagram. The cause for the decreasing stress is that the damage (microcracks) somewhere along the bar has become so high, that any increase in deformation leads to a decreasing ability to transfer stresses. Within this **damage zone** or **fracture zone** an increase in deformation takes place, at the same time as the damage increases and the transferred stress decreases.

As the stress decreases due to the increasing damage within the fracture zone, the parts outside this zone are unloaded, and they

thus contract. At the post-peak stage an increase in the total deformation corresponds to a decrease in deformation for most parts of the specimen, but an increase in the deformation within the fracture zone. The term **strain localization** is often used to characterize this behaviour. The increase in deformation is localized to the fracture zone, whereas no further increase in strain takes part outside this zone.

Another term, which is often used to describe the stress-deformation at the post-peak stage is **strain softening**, which means that the stress decreases as the average strain (or rather the deformation) increases.

In Fig. 2 the stress-deformation curves from the four gauges are shown on the assumption that the fracture zone is situated within gauge-length C. The sum of the deformations in gauges B, C and D is equal to the deformation in gauge A.

From the figure it is evident that the curves from the different gauges are different, with the exception of gauges B and D, which are equal. Thus the stress-deformation relation cannot be expressed by a single curve, as this relation depends on the gauge-length and on the position of the gauge with respect to the fracture zone. It is thus not possible to find a general stress-strain curve for a material, including the descending branch. This fact is often neglected. Many examples can be found in the litterature, where equations for such stress-strain curves for concrete have been proposed.

A general description of the stress-deformation properties can be given by means of two curves according to Fig. 3, one stress-strain (σ-ε) curve for strains smaller than the stress at the peak point, and one stress-deformation (σ-w) curve for the additional deformation w within the fracture zone, caused by the damage within this zone. The general equation for the deformation Δl on a gauge length l is then given by

$$\Delta l = \varepsilon l + w$$

where ε is taken from the σ-ε-curve and w from the σ-w-curve. The latter value is only used where there is a fracture zone within the gauge length in question. In other cases it equals zero. In the post-peak region the value of ε is taken from the unloading branch.

One essential property of the σ-w-curve is the area below the curve, as this area is a measure of the energy which is absorbed per unit area of the fracture zone during a test to failure. This value is usually called the **fracture energy** (more correct fracture energy per unit area), and is denoted by $\mathbf{G_F}$.

For the behaviour of a specimen it is of importance how much of the deformation that is due to the σ-ε-curve, and how much that is due to the σ-w-curve. In other words it is important how these curves are related to each other. One way of defining this relation is by taking the ratio between a deformation equal to G_F/f_t from the σ-w-curve and a deformation f_t/E from the σ-ε-curve. This yields a value which is called the **characteristic length $\mathbf{l_{ch}}$** of the material

$$l_{ch} = EG_F/f_t^2$$

G_F/f_t corresponds to the maximum deformation w if the shape of the curve had been a rectangle, whereas f_t/E is the maximum strain if the σ-ε-curve were a straight line, see Fig. 4. The characteristic length l_{ch} is a material property, which cannot be directly measured, but which is calculated from the measured values of E, G_F and f_t.

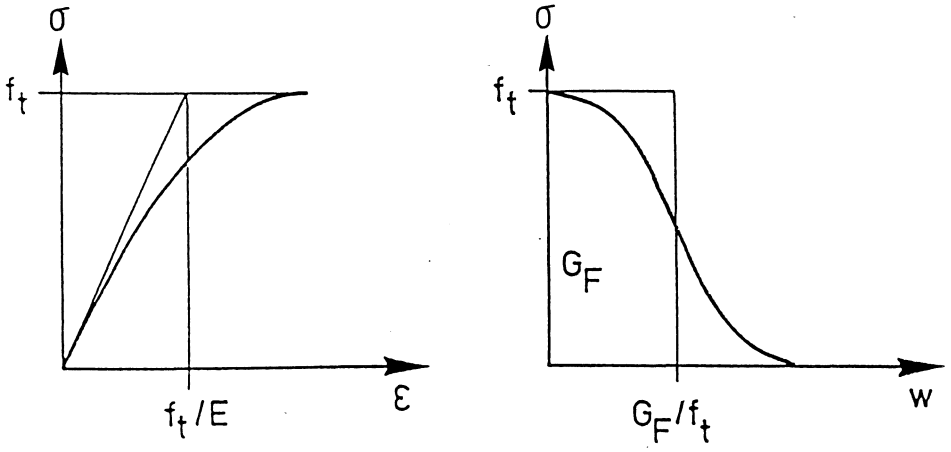

Fig. 4.

The fracture zone.

The development of the fracture zone starts by the formation of microcracks, which make this zone weaker. At this first stage the zone may comprise a certain length in the stress direction, and the additional deformation corresponds to the the sum of the additional deformations within these microcracks.

As the deformation increases, it gets more and more localized, and in reality practically all the additional deformation happens within a narrow zone, which may best be described as an irregular crack, which changes direction, bifurcates etc, depending on the inhomogenities of the material. Thus the width of the fracture zone (the size in the stress direction) can be assumed to be practically zero.

One way of expressing this is simply to assume as a formal model that the fracture zone is a crack with the width w and with the ability to transfer stresses according to the σ-w-curve. A crack with the ability to transfer stresses is of course no real crack, but just a hypothetical model. It can therefore be said that the crack is "fictitious". This model has been called the "fictitious crack model". The model was first published by Hillerborg et al (1976), and it has later been further developed and applied in many publications, e g by Petersson (1981) and Gustafsson (1985).

However from the point of view of practical application it does not matter whether the additional deformation in the fracture zone is assumed to take part in a "fictitious crack" or if it is assumed to be distributed on a certain length, as long as this length is small in comparison with other dimensions of the structure. Thus there is hardly any practical difference between the "fictitious crack model", and the "crack band model" proposed by Bazant and Oh (1983), where they assume a distribution on a length equal to 3 times the maximum aggregate size. These models are often implemented into a finite element scheme in different ways, but this is another question, which will be commented upon later.

The concentration of the fracture zone to a thin band or a single crack is typical for tensile fracture of concrete. It is not accompanied by any significant lateral deformations or stresses, and thus it corresponds to a very simple one-dimensional stress and deformation state. Therefore the σ-w-curve can be assumed to be a material property, which is rather insensitive to the shape of the structure and the general stress state, as long as all other stresses (e g a possible perpendicular compressive stress) are low compared to the strength.

For metals the stress state is much more complicated, as the yielding of metals gives rise to a complicated three-dimensional stress state and lateral deformations. Fracture mechanics of metals cannot be treated with the same model that is used for concrete.

For concrete in compression the fracture zone also develops in another way than in tension, as crushing is accompanied by lateral deformations. The compression fracture is much more complicated than tensile fracture. Some kind of descending σ-w-curve exists, but probably it cannot be regarded to be a well defined material property. The maximum stress as well as the shape of the curve can be expected to depend on e g confinement through stirrups or strain gradients. The application of the fracture mechanics ideas to compressive fracture is still an unexplored but interesting domain. It will only be very shortly commented upon at the end of this paper.

Material properties.

The stress-strain curve in tension for ordinary concrete deviates rather little from a straight line. Thus for most practical applications this relation can be assumed to be a straight line. All applications so far seem to have been based on this assumption.

The stress-deformation curve corresponding to the descending branch can be measured by means of modern test equipment. The shape of this curve is now relatively well known. It has the general shape shown in Fig. 5. One important parameter of the curve is the enclosed

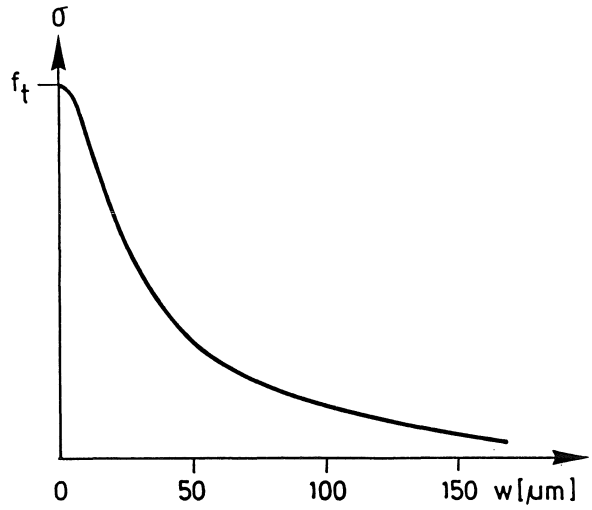

Fig. 5. Ordinary shape of the σ-w-curve for concrete.

area, which equals the fracture energy G_F. Another important property may be the initial slope of the curve. This property and its practical significance has not hitherto been studied in detail.

The fracture energy G_F can suitably be determined by means of a simple bending test on a notched beam according to a RILEM recommendation, Fig. 6. The load-deformation curve is recorded in the test. The total energy, that is absorbed during the test, is equal to the sum of the areas A_1, A_2 and A_3. A_1 is measured in the diagram, A_2 is calculated as $F_1 \cdot \delta_o$, where F_1 is a central force giving the same bending moment as the weight of the beam and the loading equipment. A_3 is assumed to be equal to A_2. This total energy is divided by the area b(h-a), that has been fractured, in order to get the value of G_F.

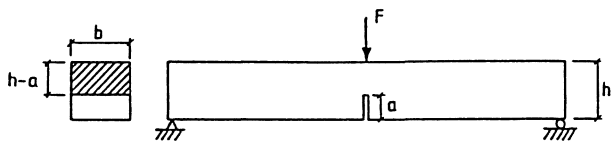

Fig. 6. Test for the determination of the fracture energy G_F according to RILEM Recommendation (1985).

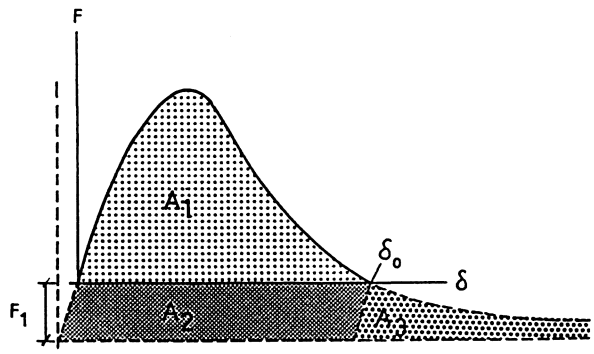

For normal concrete qualities the material parameters are within the following ranges:

$E = 20 - 40$ GPa
$G_F = 65 - 200$ N/m
$f_t = 2 - 4$ MPa
$l_{ch} = 0.1 - 1$ m

The value of l_{ch} can be expected to be lower for high strength concrete and for light weight concrete than for ordinary concrete, which means that these materials are more brittle.

For fibre reinforced concrete the shapes of the σ-ε- and σ-w-curves may differ much from those for plain concrete. These curves then have to be determined and introduced into the analyses for the particular materials in question.

Application, principles.

Wherever tensile strains appear, which tend to pass the strain corresponding to the peak point in the tensile stress-deformation curve, a fracture zone starts to develop. Then the model outlined above can be applied, which means that the σ-w-curve is applied to the additional deformation in the fracture zone.

Let us as an example look at the bent beam in Fig. 7. At low loads the simple beam theory can be used, which means that the strains and stresses vary linearly across the section, with a maximum stress equal to

$$\sigma_{max} = 6M/bd^2$$

where M is the acting moment, b the width and d the depth of the beam. When the maximum stress reaches the tensile strength f_t a fracture zone starts developing if the deflection of the beam is increased. As the deflection increases, the fracture zone grows into

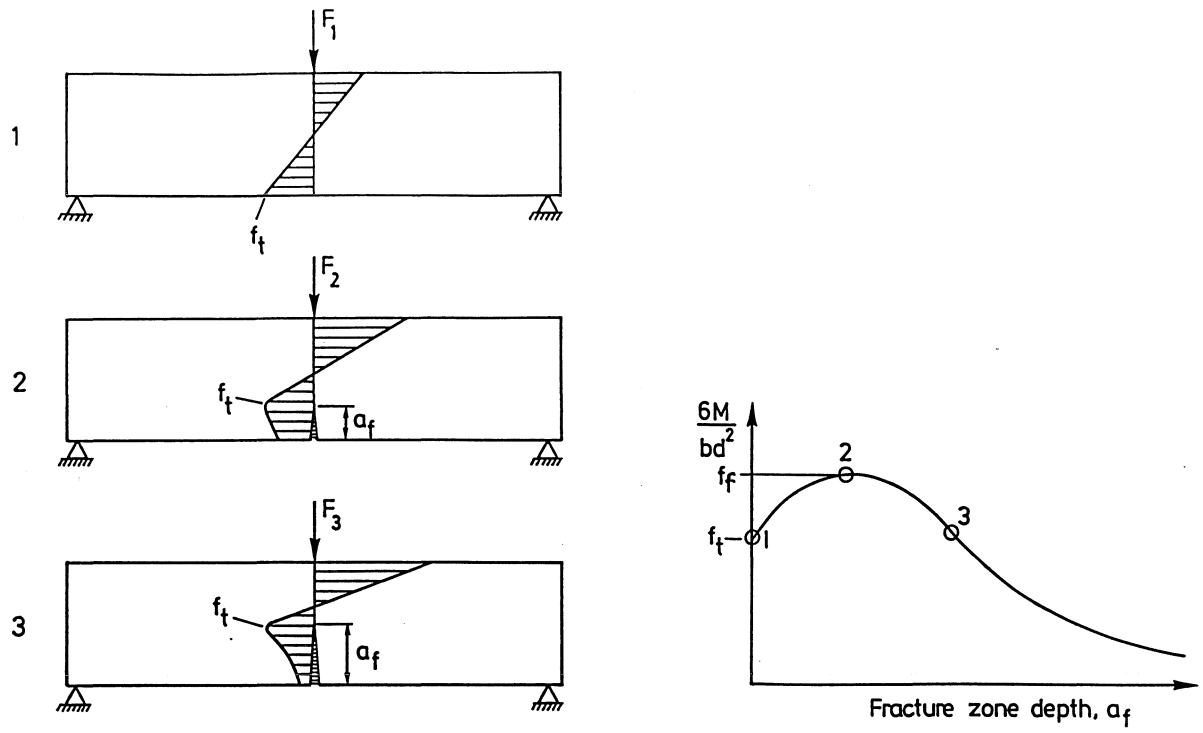

Fig. 7. Stress development in an unnotched beam.

the beam. At the same time the stress across this zone decreases, as the additional deformation increases. At the upper end of the fracture zone the stress is equal to f_t.

By means of a suitable numerical analysis the development of the stress distribution in the beam can be followed as the fracture zone grows. The corresponding development of the bending moment can be calculated, as it is shown in Fig. 7, as well as the deflection.

Exactly the same procedure can be followed also if the beam contains a crack from the beginning, Fig. 8, which is the case treated by conventional fracture mechanics. In that case the fracture zone start to grow already as soon as a load is applied, due to the stress concentration at the crack tip. The growth is however slow in the beginning. It can be shown that the depth of the fracture zone at low loads in this case is approximately proportional to the square of the moment.

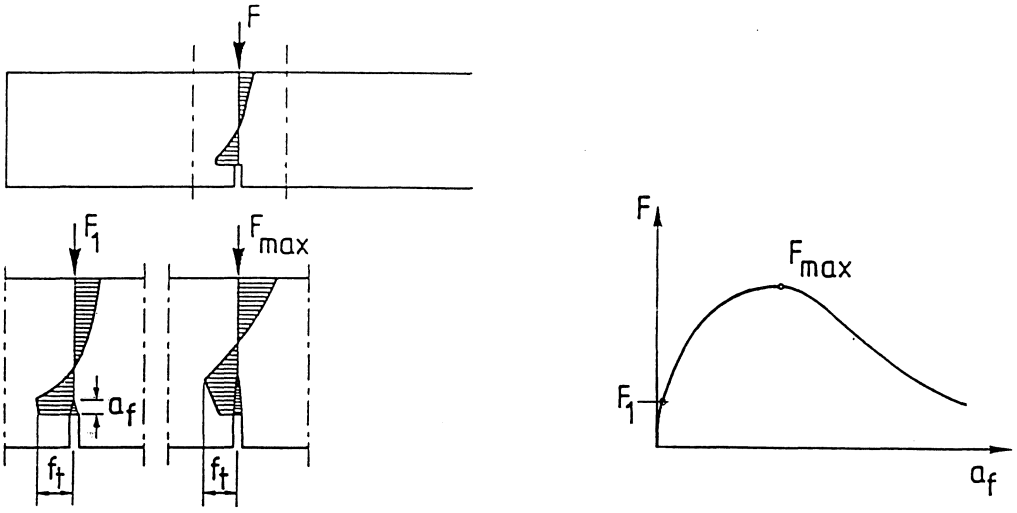

Fig. 8. Stress development in a notched beam.

In more complicated cases it is possible that the fracture zone starts inside a structure and grows in two directions. This may for instance happen with some shear cracks in reinforced beams or with splitting cracks under concentrated forces, like end anchors for prestressing tendons.

Size parameters. Brittleness number.

The characteristic length l_{ch} is a material property. If a characteristic size of a structure is divided by l_{ch}, this gives a dimensionless ratio, which relates a property of the structure to a property of the material. For a beam the depth d is often chosen as the characteristic size, and the ratio then is d/l_{ch}. This ratio is sometimes called **brittleness number**, as it gives an indication of the brittleness of the structure. The higher the brittleness number, the more brittle the structure.

As will be demonstrated later, the relative strength of a structure, expressed as a ratio between a formal stress at maximum load and f_t, is a function of d/l_{ch}. In this way many results of the theoretical analyses can be given in dimensionless general diagrams.

Application by means of finite element analysis.

The application by means of the finite element method (FEM) is rather straightforward if the fracture zone follows the direction of the element boundaries. The fracture zone then can be modelled either as a separation between elements (the fictitious crack model) or as a change in stress-strain properties of a row of elements (the crack band model).

In the fictitious crack model it may for instance be suitable to calculate the forces in the node points between the elements. When such a force reaches a value corresponding to the tensile strength, a separation between the elements is assumed, Fig. 9. Forces are introduced between the separated node points. The values of these forces depend on the separation distances w according to the σ-w-curve for the material, see Fig. 3. In this way the development of the fracture zone and the corresponding forces and deformations can be followed.

In the crack band model the formal stress-strain-curve for an element, where the fracture zone passes, is simply determined according to the general formula

$$\varepsilon_1 = \varepsilon + w/l$$

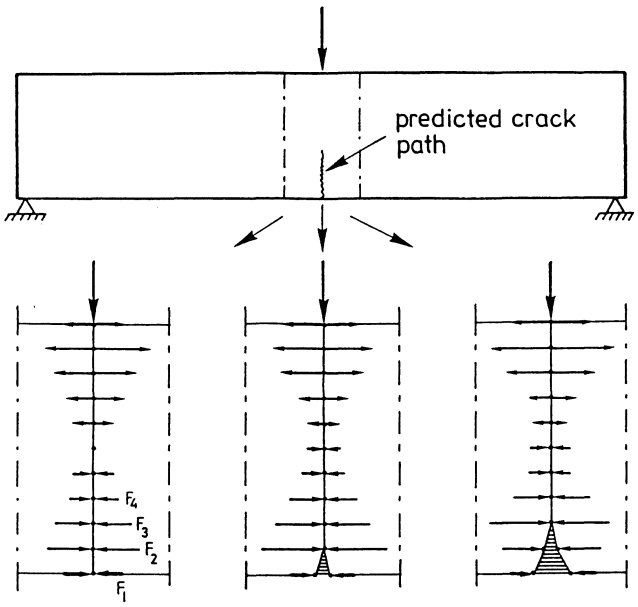

Fig. 9. The formation and growth of a fracture zone, modelled by means of a successive separation of node points.

where ε_1 is the formal average strain in the element, ε and w are in accordance with the properties of the material, and l is the size of the element in the direction of the tensile stress.

In the types of analyses described above, the fracture zones and the cracks propagate along discrete cracks or bands. Therefore this type of approach is called the **discrete crack approach**. This approach is more difficult to apply when the fracture zone does not follow along the direction of the element boundaries, but crosses the elements at skew angles. Certain possibilities exist for the application of the discrete crack approach to such cases, but these are complicated, and will not be discussed here.

When the direction of the fracture zone does not follow along the element boundaries it is easier to apply the **smeared crack approach**. In this approach a formal stress-strain relation is assumed for the material, just like in the crack band model described above. Even though this approach may be formally easier to apply, it involves some problems and risks of misinterpretations.

When the formal stress-strain relation shall be calculated the value of the length l is not well defined when the direction of the tensile stress forms a skew angle with the element directions. This leads to an uncertainty in the determination of this relation, which gives rise to an uncertainty in the results.

Still worse, however, is that the properties of many types of finite elements are not suitable for describing the growth of a fracture zone in a realistic way. When the strain in an element reaches the descending branch in the stress-strain curve, this corresponds to a negative modulus of elasticity for further deformations. Such an element may then be coupled more or less in parallell with an adjoining element with a positive modulus of elasticity. The result may be very discontinuous stress and strain distributions, which are unrealistic. In order to avoid large mistakes it is necessary to be very careful when the smeared crack approach is used. An uncritical application may lead to quite unreliable results. After this warning

has been given, the smeared approach will not be discussed any further in this paper.

Application to the bending of beams.

All the results which will be shown beolw are based on the application of the fictitious crack model. The assumed σ-ε-relation is always a straight line, whereas two different relations have been used for the σ-w-relation according to Fig. 10. The single straight line, denoted "SL", is the simplest possible assumption for the numerical analyses, whereas the bilinear relation is meant to be a good approximation for the real shape. It is denoted "C" for concrete.

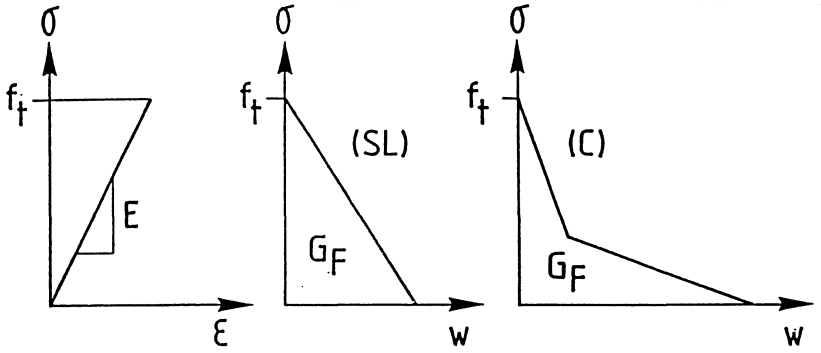

Fig. 10. Simplified assumptions regarding material properties.

A simple example is the bent unreinforced beam, without or with a notch (crack) on the tensile side. Figs. 11-14 show results of such analyses. The strength of the beam is expressed as a formal bending stress at failure, for the unnotched beam

$$f_f = 6M/bd^2$$

and for the notched beam

$$f_{net} = 6M/b(d-a)^2$$

where M is the maximum moment and a is the notch depth.

The value of the ratio f_f/f_t can be taken from diagrams of the type shown in Fig. 7, and the ratio f_{net}/f_t from Fig. 8.

Fig. 11 shows the variation of the flexural strength (modulus of rupture, MOR) with d/l_{ch}. From this diagram it can e g be seen that the ratio between flexural strength and tensile strength for a 100 mm deep beam with l_{ch} = 400 mm can be expected to be about 1.6, which is in a reasonable agreement with experience.

With the model it is also possible to study the influence of shrinkage stresses. Fig. 12 shows an example of this, where the shrinkage strains have been assumed to have values of an order which can be expected in a normal interior structure.

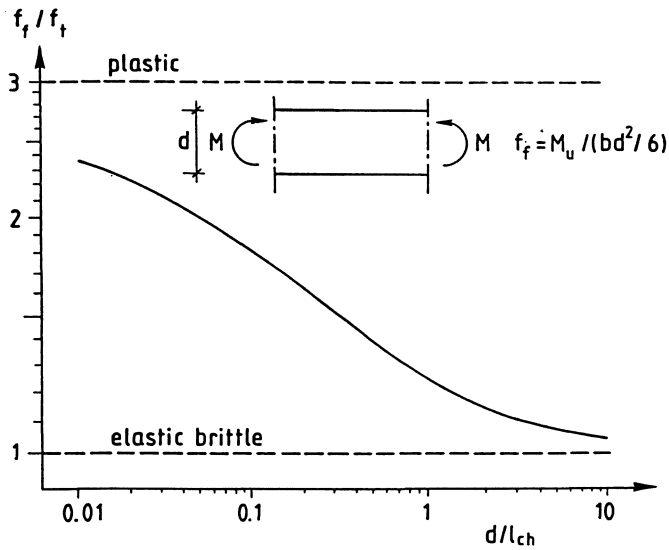

Fig. 11. Ratio between flexural strength and tensile strength.

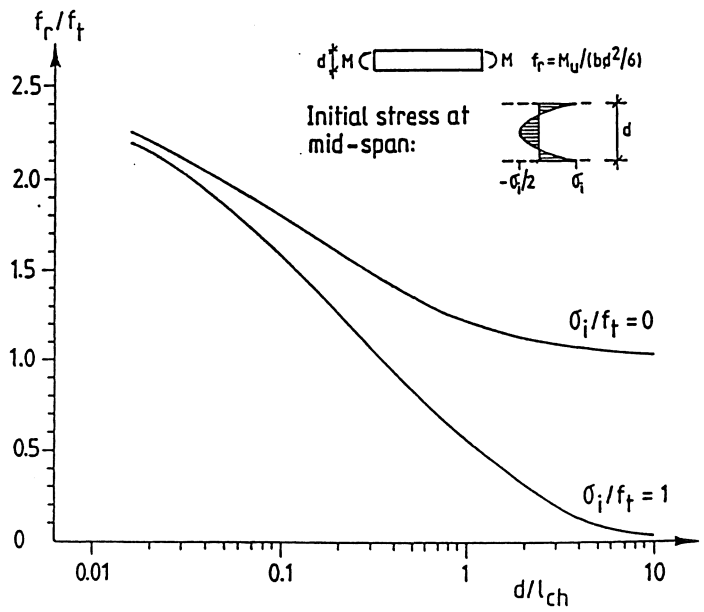

Fig. 12. Influence of shrinkage stresses on the ratio between flexural strength and tensile strength.

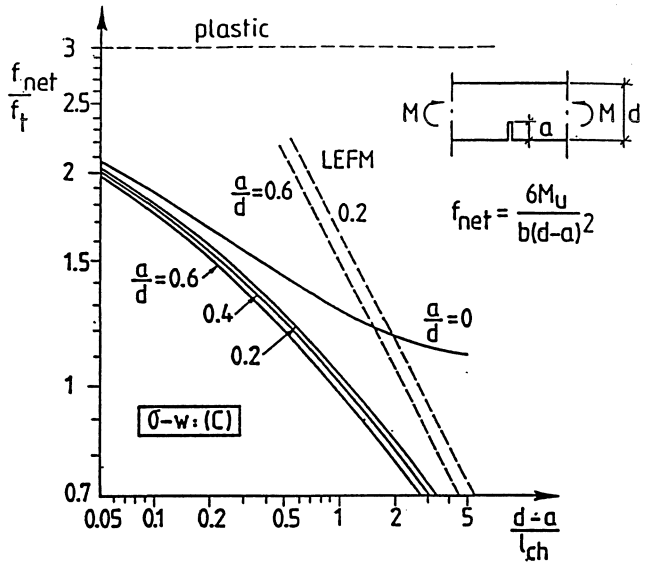

Fig. 13. Ratio between net bending strength of a notched beam and the tensile strength.

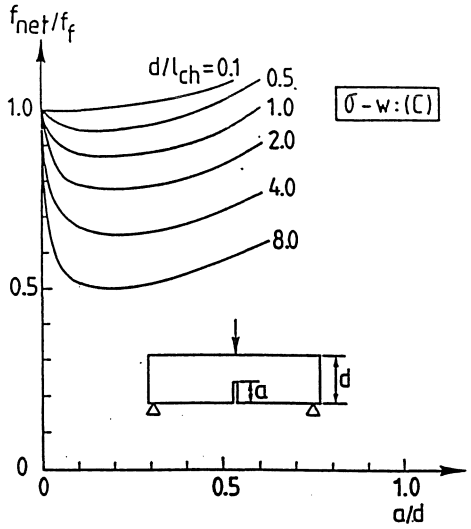

Fig. 14. Influence of the notch depth on the net bending strength.

Fig. 13 shows the variation of the strength of a notched beam with d/l_{ch}. In this case the strength is very sensitive to the depth for deep beams. As a matter of fact the strength for deep beams approaches values which are predicted by linear elastic fracture mechanics, which means that they are inversely proportional to the square root of the beam depth.

Fig. 14 shows how the depth of the notch influences the net bending strength of a notched beam. For a low value of d/l_{ch} the notch has practically no influence on the net bending strength f_{net}, which is nearly the same as the bending strength f_f of an unnotched beam. These beams are said to be notch insensitive. For high values of d/l_{ch} the value of f_{net} decreases as soon as there is a notch, which means that these beams are notch sensitive. It can be noted that the **notch sensitivity** is not a material property, but a property that depends on the beam depth d as well as on the material property l_{ch}.

In all the figures it can be seen that the strength depends on the size d of the beam. Thus there is a **size effect**, which is explained by means of the fracture mechanics approach. The size effect is greater for notched beams than for unnotched, particularly for deep notched beams. For unnotched beams this size effect increases when shrinkage or temperature stresses are acting.

In Figs. 11 and 13 it can be seen that the strength approaches the value predicted by the theory of plasticity for small beams, and that it approaches the value predicted by the theory of elasticity for large beams. The analysis covers all cases between these extremes for unnotched as well as notched beams. It thus has a general applicability. A small value of the "brittleness number" d/l_{ch} gives a more plastic-tough behaviour, whereas a high value gives a more elastic-brittle behaviour.

Sensitivity analysis.

The formal strength according to the above results depends on the value of d/l_{ch}, where l_{ch} in its turn depends on E, G_F snd f_t according to the relation $l_{ch} = EG_F/f_t^2$. The diagrams are given in logaritmic scales (except Fig. 12). For a small change in d/l_{ch} the relation can approximately be written

$$\ln(f_f/f_t) = A - B\ln(d/l_{ch}) = A - B\ln(df_t^2/EG_F)$$

$$\ln f_f = A + (1-2B)\ln f_t - B\ln d + B\ln E + B\ln G_F$$

where A and B are constants, with B showing the negative slope in the diagram at the studied part of the curve.

A differentiation gives

$$\frac{df_f}{f_f} = (1-2B)\frac{df_t}{f_t} - B\frac{dd}{d} + B\frac{dE}{E} + B\frac{dG_F}{G_F}$$

This expression shows the relative change in the formal strength f_f for a small relative change in one of the parameters. This can be called the **sensitivity**, and it is determinded from the slope -B in the diagrams. It must be noted that the diagrams are given with the scale on the vertical axes 4 times as large as the scale on the horizontal axis. Therefore the slopes, which are measured in the figures, must be divided by 4. If for example the measured slope is -0.6, the value of B is 0.15, which means that the sensitivity with regard to G_F is 0.15 and with regard to f_t 0.7. In this case an increase in f_t with 10 percent increases f_f with 7 percent, whereas an increase in G_F with 10 percent increases f_f with 1.5 percent. In the same case an increase in the beam depth d with 10 percent decreases f_f with 1.5 percent.

Application to unreinforced concrete pipes.

An interesting practical application has been made to the strength of unreinforced concrete pipes. For these there are essentially two different types of failure, that are of interest, see Fig. 15. One is the bending failure (or beam failure), where the pipe is supported and loaded like a beam. The other is the crushing failure (or ring failure), where the pipe is loaded and supported along its length. This type of load results in bending failures in sections along the pipe, at the top and the bottom, and at the two sides. The structure is under these conditions statically indeterminate, which means that a moment redistribution can take place before the maximum load is reached. The amount of this moment redistribution depends on the toughness of the structure, and therefore increases with a decrease in size.

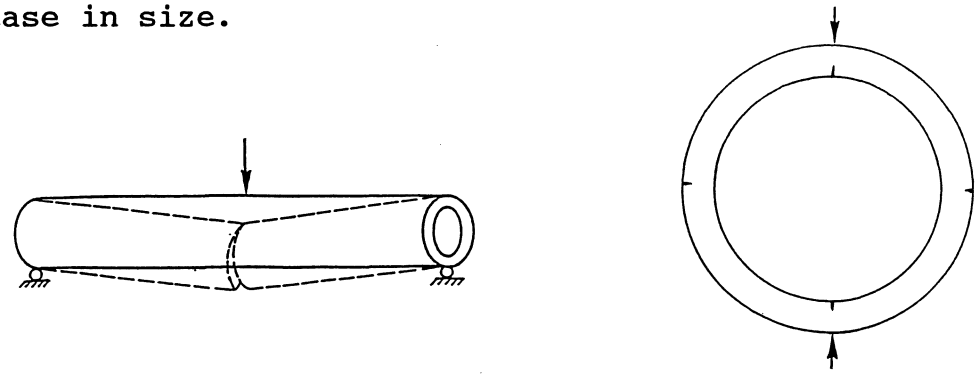

Fig. 15. Bending failure and crushing failure of a pipe.

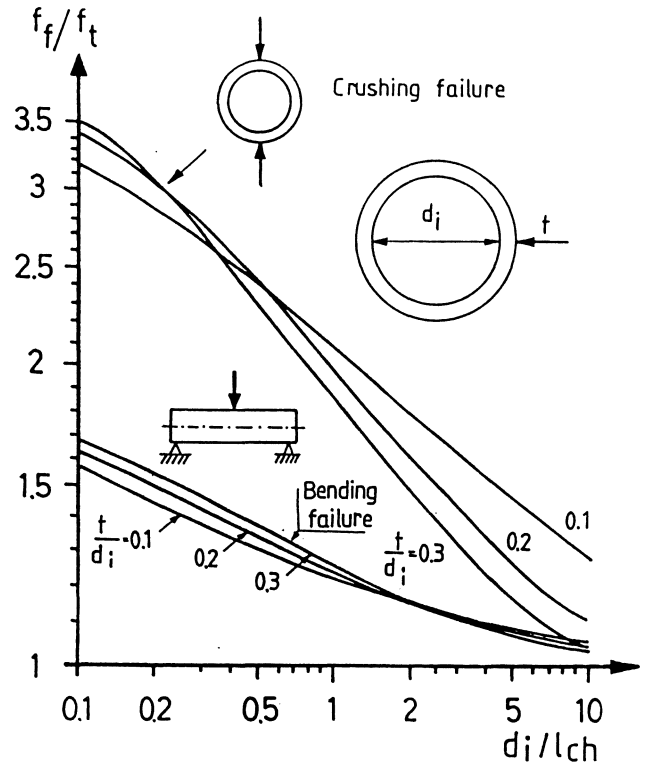

Fig. 16. Variation of formal bending strength of a pipe.

In Fig. 16 the variation in the formal bending strength with the size of the pipe is shown for these two loading situations. The formal strength f_f is the maximum stress at maximum load, calculated according to the theory of elasticity.

From the figure it is evident that the formal strength is much higher for the crushing failure than for the beam failure. The size dependence is also much higher for the crushing failure. The reason for the difference in strength is that the section depth for the acting moment is much lower for the crushing failure (the wall thickness) than for the beam failure (the diameter of the pipe). The reason for the higher size dependence for the crushing failure is that this structure is statically indeterminate.

The values according to Fig. 16 are in a good agreement with test results. They have found a practical application for redesign of certain pipes.

Application to shear failure of beams.

The shear strength of reinforced beams without shear reinforcement has also been analysed by means of the fictitious crack model. This is a very complicated case, as it depends not only on the concrete properties in tension, but also on concrete properties in compression and shear, on the steel properties, on the bond behaviour between concrete and steel, and on many other factors. The fracture zone and the resulting cracks are curved, and they can appear in many different positions.

Due to the complexity of the shear fracture the analysis which has been performed so far has had to be performed on the basis of many approximations and simplifications. Thus only one crack at a time has been studied, but this crack has been varied in order to find the most dangerous situation. The shape and position of the crack has been assumed in advance for each calculation, but afterwards it has been checked that the crack is nearly perpendicular to the principal tensile stress. Dowel action has not been taken into account, nor aggregate interlock. The properties of the reinforcement, bond properties, and failure in the concrete compression zone have been taken into account.

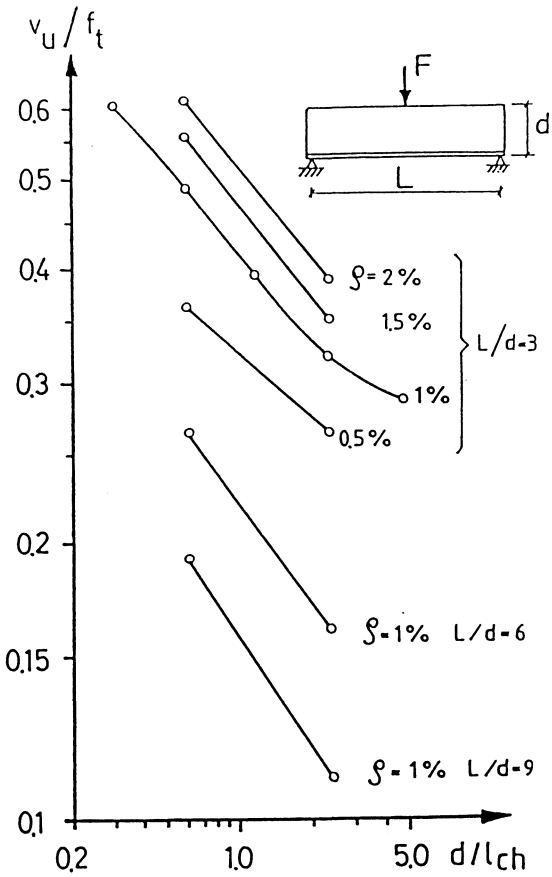

Fig. 17. Theoretical ratio between formal shear strength and tensile strength for a beam with longitudinal reinforcement.

The results of the analyses are shown in Fig. 17. The variables have been the depth (expressed as d/l_{ch}), the span to depth ratio, and the reinforcement ratio ρ. Of a special interest is the influence of the beam depth, which is wellknown from tests, but which has not earlier had any rational explanation.

A very large number of tests have been performed regarding the shear strength of beams, and as a matter of fact all our knowledge, as expressed in building codes and text books, is based on these tests. As we now for the first time have a pure theoretical analysis of the shear failure, it is interesting to compare this with test results and with the code formulas. Such comparisons are shown in Figs. 18 - 20. As all the material parameters in the tests are not known, particularly not the fracture enegy G_F, it has only been possible to make relative comparisons, which means that all curves in a diagram have been drawn through one common point.

From all the figures it is evident that the theoretical results are in a good agreement with the test results. Regarding the influence of beam depth and reinforcement ratio they are also in a good agreement with the CEB Model Code, which is mainly based on the same test results. The ACI code does not show any good agreement with the theoretical results or the test results.

In Japan (Iguro et al, 1984) a test series has been performed, where the beam depth has been varied between 0.1 m and 3 m, i e by a factor of 30. From these tests it was concluded that the shear strength is inversely proportional to the fourth root of the depth. This corresponds to a 45° slope in Fig. 17, and it is thus in a good agreement with the theoretical results.

Based on the theoretical analysis and the test results it can approximately be assumed that the following equation is valid for a beam with a constant span to depth ratio and a constant reinforcement ratio:

$$v_u/f_t = k(d/l_{ch})^{-1/4} = k(l_{ch}/d)^{1/4}$$

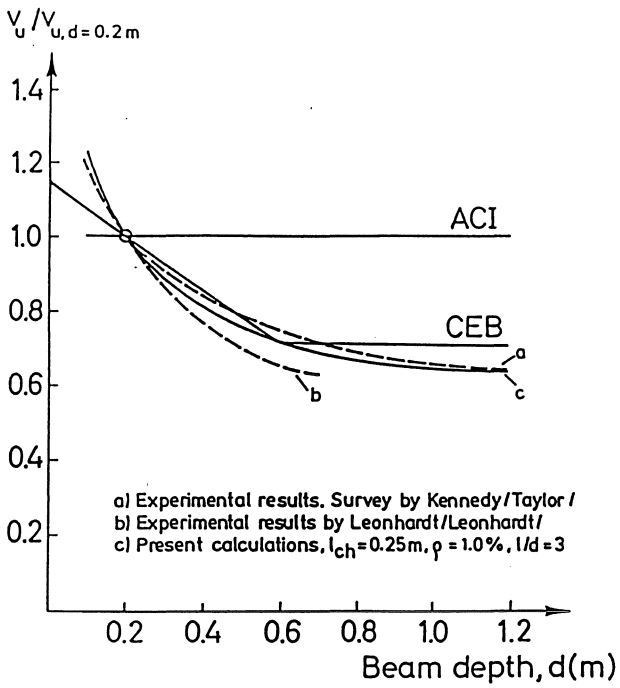

Fig. 18. Influence of beam depth.

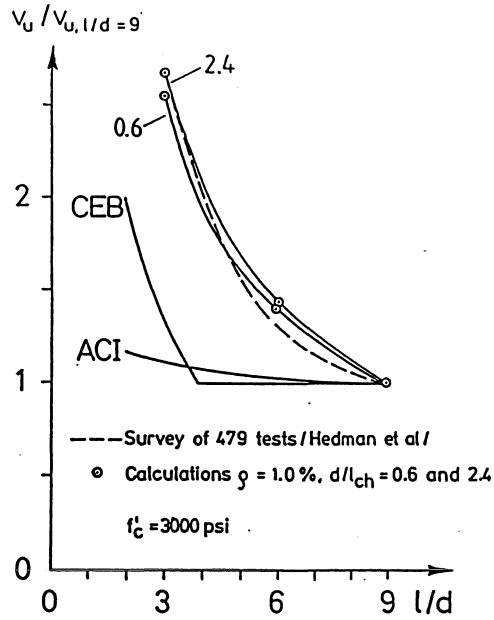

Fig. 19. Influence of span to depth ratio.

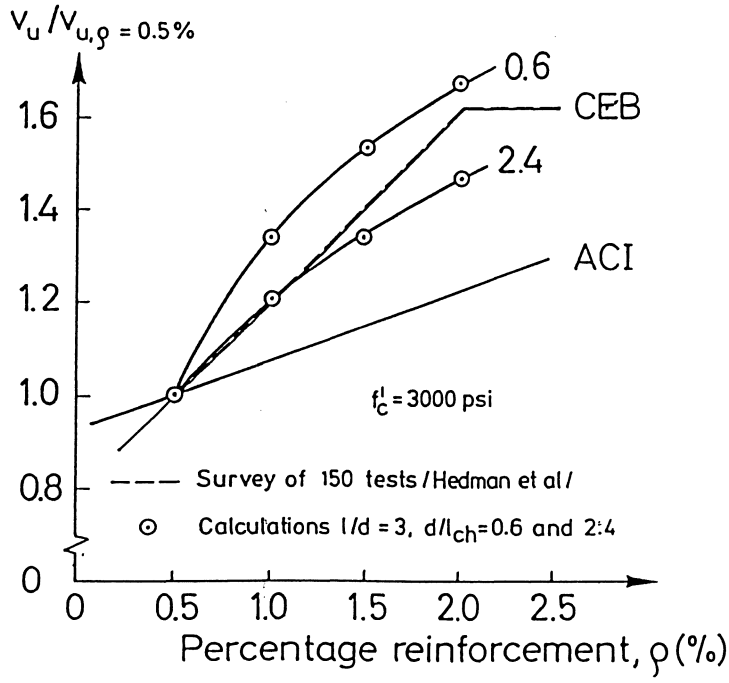

Fig. 20. Influence of reinforcement ratio

Figs. 18 - 20. Comparisons between theoretical values, test values and code values regarding the influence of different factors on the shear strength of reinforced beams.

where v_u is the formal shear strength (shear force divided by the cross section area) and k a constant. This expression can be rearranged by inserting the definition $l_{ch} = EG_F/f_t^2$:

$$v_u = kf_t(EG_F/df_t^2)^{1/4} = k(EG_Ff_t^2/d)^{1/4}$$

From this expression it can be seen that the shear strength depends as much on G_F as on f_t^2. It is generally accepted that the tensile strength f_t is approximately proportional to the square root of the compressive strength. Thus f_t^2 can be assumed to be proportional to the compressive strength. The conclusion from this is that the shear strength of a beam depends as much on the fracture energy of the concrete in the beam as on its compressive strength.

When a laboratory test is performed on a concrete structure, the compressive strength is traditionally always measured and reported. From the above it follows that the fracture energy should also be measured and reported where shear tests are performed, as this property is as important as the compressive strength. The same may hold also for many other types of structural tests.

Also in code formulas for shear strength the fracture energy ought to be taken into account in some way or other. How this should be done is too early to specify, but one possibility could be to give some type of correction factor, depending on the type of concrete, for example reduction factors for light weight concrete and for high strength concrete.

Direction of future research.

It has been demonstrated above that the application of fracture mechanics to concrete structures can give important contributions to the understanding of the behaviour of structures in cases where our knowledge earlier has been mainly based on empirical studies, like the ratio between flexural and tensile strength, the influence of shrinkage on the flexural strength and the shear strength of beams.

Still we are however only in the beginning of a development. If we for example look on the application to shear fracture, the results which were demonstrated are based on analyses where many rather rough approximations have been made. These were partly due to a lack of knowledge, e g regarding the aggregate interlock and the dowel action, and partly on the complexity of the problem, which made it too difficult to take all factor into account with the existing finite element program.

Thus one important type of research is to find more adequate material properties to be inserted into the finite element analyses. One example of such a research work is mentioned below.

An other important type of research is to develop finite element programs, which are better adopted to handle this type of fracture mechanics, with localization of fracture zones and strain softening.

It is also important to apply the model in a systematic way to real structures in order to achieve a better understanding of different types of behaviour, e g as a background for better design rules and codes. The results of such systematic analyses can preferrably be given in dimensionless general diagrams of the types shown above.

Present research in Lund (spring 1988).

A large test program is going on regarding the behaviour of a fracture zone in mixed mode, i e with shear deformations and stresses in a fracture zone after it has started in tension. Some results were presented in 1987. More systematic results will be presented at a conference in Vienna in July 1988, and the final complete report is expected to appear in 1989. One example of a test result is presented in Fig. 21.

A first attempt has also been made to apply the model with localization and strain hardening to the fracture in the compression zone of

a reinforced beam. These first results indicate that the stress-strain relation to be used for the practical design should preferrably have an ultimate strain equal to k_1/x, instead of the normally assumed 3.5 permille, where k_1 is a material property and x is the depth of the compression zone. If this conclusion is correct, it will have a significant influence in many practical situations. Further research is needed before the result is sufficiently confirmed.

In a third project a number of tests are being performed on some simple unreinforced structures in order to check the general applicability of the fracture mechanics aproach. A wide range of different materials are tested, particularly with respect to different toughness. Very brittle materials are tested, like pure cement paste, as well as wery tough materials, like fibre reinforced concrete, and some materials in the intermediate range.

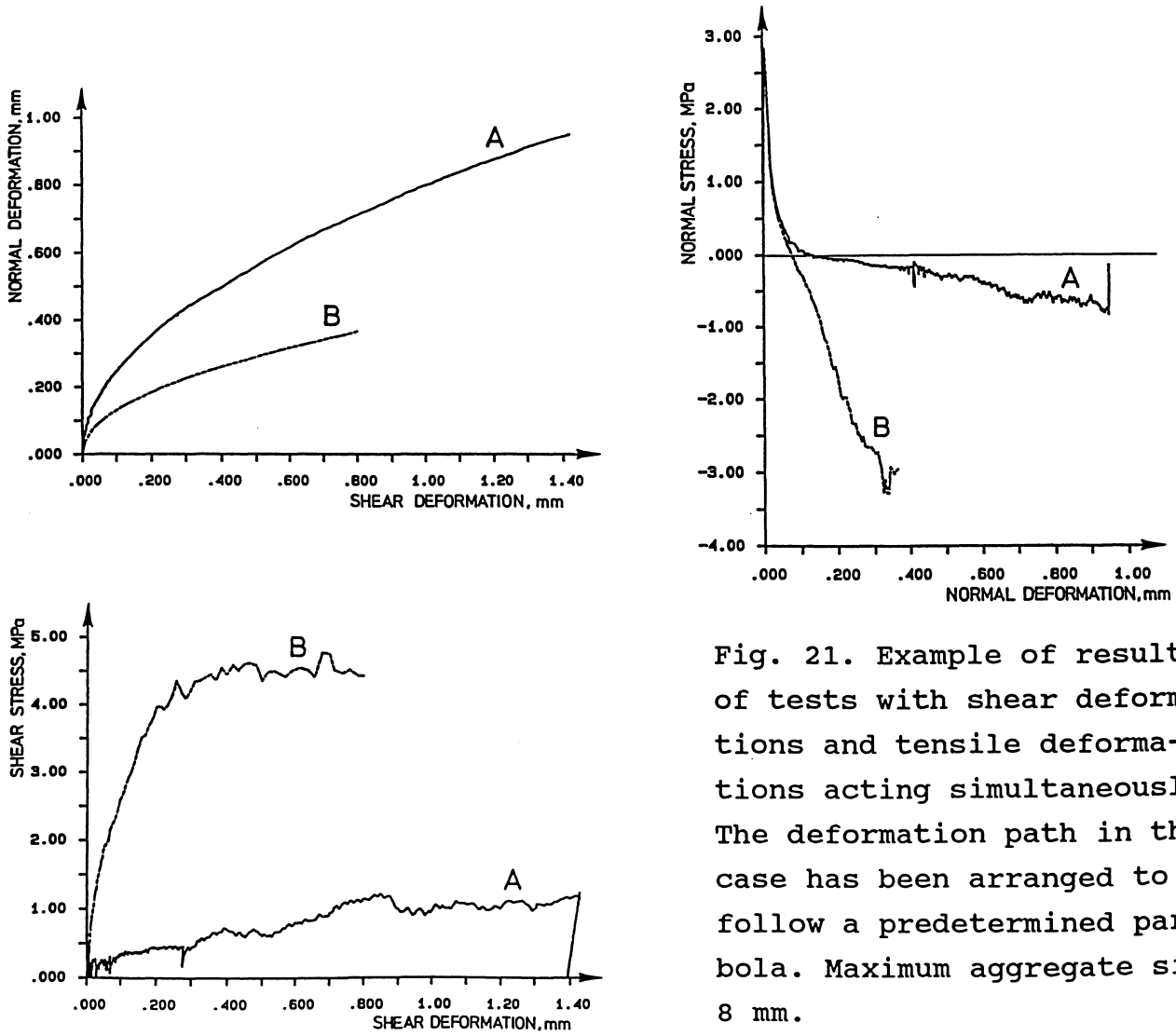

Fig. 21. Example of results of tests with shear deformations and tensile deformations acting simultaneously. The deformation path in this case has been arranged to follow a predetermined parabola. Maximum aggregate size 8 mm.

References

American Concrete Institute (1983) Building code requirements for reinforced concrete, ACI 318-83.

Bazant, Z.P. and Oh. B.H. (1983) Crack band theory for fracture of concrete. RILEM, Materials and Structures, Vol 16, No 93, 155-177.

CEB/FIP Model Code for Concrete Structures (1978). CEB Bulletin 124/125-E.

Hillerborg, A., Modéer, M. and Petersson, P.E. (1976) Analysis of crack formation and crack growth in concrete by means of fracture mechanics and finite elements. Cem. and Concre. Res., 6, 773-782.

Iguro, M., Shioya, T., Nojiri, Y. and Akiyama, H. (1984) Experimental studies on shear strength of large reinforced concrete beams under uniformly distributed load (in Japanese), Proceedings, Japan Society of Civil Engineers (Tokyo), No. 348/V-1, Aug. 1984, 175-184. Also Concrete Library International, JSCE, No. 5, Aug. 1985, 137-154 (in English).

Gustafsson, P.J. (1985) Fracture mechanics studies of non-yielding materials like concrete. Report TVBM-1007, Div. of Building Materials, Lund Inst. of Technology, Sweden.

Petersson, P.E. (1981) Crack growth and development of fracture zones in plain concrete and similar materials. Report TVBM-1006, Div. of Building Materials, Lund Inst. of Technology, Sweden.

RILEM (1985) Determination of the fracture energy of mortar and concrete by means of three-point bend tests on notched beams, RILEM, Materials and Structures, Vol 18, No 106, 185-290.